CHEMISTRY
A EUROPEAN JOURNAL

DOI: 10.1002/chem.200903505

Magnetic Properties of Two New Fe_4 Single-Molecule Magnets in the Solid State and in Frozen Solution

Christoph Schlegel,[b] Enrique Burzurí,[c] Fernando Luis,[c] Fabrizio Moro,[a] Maria Manoli,[d] Euan K. Brechin,[d] Mark Murrie,[e] and Joris van Slageren*[a, b]

Abstract: Two novel tetranuclear, star-shaped iron(III) clusters, $[Fe_4(acac)_6(Br\text{-}mp)_2]$ and $[Fe^{III}_4(acac)_6(tmp)_2]$, are described. Both have $S=5$ ground states resulting from antiferromagnetic nearest-neighbour superexchange interactions, with $J=-8.2\ cm^{-1}$ and $J=-8.5\ cm^{-1}$ for **1** and **2**, respectively. Energy barriers for the relaxation of the magnetisation of approximately $12\ cm^{-1}$ were derived from AC susceptibility measurements. Magnetic resonance measurements revealed a zero-field splitting parameter $D=-0.34\ cm^{-1}$ for both complexes. AC susceptibility measurements in solution demonstrated that the complexes are reasonably stable in solution. Interestingly, the magnetisation relaxation slows down significantly in frozen solution, in contrast to what is generally observed for single-molecule magnets. This was shown to result from a large increase in τ_0, the prefactor in the Arrhenius equation, with the energy barrier remaining unchanged.

Keywords: cluster compounds · EPR spectroscopy · magnetic properties · magnetisation relaxation · molecular magnetism

Introduction

The properties of single-molecule magnets (SMMs) in the solid state have been studied in great detail over the past two decades and are now very well known.[1] The isotropic superexchange coupling between the ions is such that the spin ground state has a large spin (typically $S \geq 4$). The combined zero-field splitting of the ions leads to a net uniaxial magnetic anisotropy for the molecular spin, which generates an energy barrier between the spin-up and spin-down configurations. The result is that these systems show slow relaxation of the magnetisation at low temperatures. In addition, single-molecule magnets show pronounced quantum effects, such as quantum tunneling of the magnetisation.[1] The organic ligand shell shields the magnetic core from the surroundings and, to a first approximation, the molecular properties are independent of these. In spite of that, magnetic dipolar interactions between molecules can lead to long-range dipolar magnetic ordering,[2] and are also thought to be responsible for the observed lack of selection rules in quantum tunneling.[3] The large majority of studies on SMMs have been carried out on (micro)crystalline samples. However, investigating the properties of these systems in conditions other than the (micro)crystalline state is becoming increasingly important for the following reasons: first of all, observation of slow relaxation of the magnetisation in samples of frozen solutions or similar matrices is the ultimate proof of SMM behaviour. Thus, whereas the onset of an out-of-phase signal in the AC susceptibility is often taken as an indication of SMM behaviour, it may actually be the onset of long-range ordering,[4] spin-glass-like behaviour,[5] or the phonon bottleneck effect.[6] Secondly, any viable application for molecular nanomagnets will involve their deposition on surfa-

[a] F. Moro, Dr. J. van Slageren
School of Chemistry
University of Nottingham
Nottingham, NG7 2RD (UK)
Fax: (+44) 1159513563
E-mail: slageren@nottingham.ac.uk

[b] Dr. C. Schlegel, Dr. J. van Slageren
1. Physikalisches Institut
Universität Stuttgart
Pfaffenwaldring 57, 70550 Stuttgart (Germany)

[c] E. Burzurí, Dr. F. Luis
Instituto de Ciencia de Materiales de Aragón
CSIC-Universidad de Zaragoza
50009 Zaragoza (Spain)

[d] Dr. M. Manoli, Dr. E. K. Brechin
School of Chemistry
University of Edinburgh
West Mains Road, Edinburgh, EH9 3JJ (UK)

[e] Dr. M. Murrie
Department of Chemistry,
The University of Glasgow
University Avenue Glasgow G12 8QQ (UK)

ces. Whereas the archetypical SMM Mn_{12} was shown to be relatively unstable on surfaces,[7] Fe_4 derivatives retain SMM properties.[8] Thirdly, SMMs are currently showing great promise for the study of mesoscopic quantum coherence,[9] where a high degree of dilution has a strongly favourable effect on coherence times. Studies have shown that SMM properties are sometimes unaffected in frozen solution, but in most cases the performance of SMMs deteriorates significantly in noncrystalline environments.[10]

Here, we present two novel tetranuclear star-shaped iron(III) clusters together with an in-depth investigation of their magnetic properties. Interestingly, we find that the relaxation time of the magnetisation increases on going from the solid state to frozen solutions, in contrast to what has thus far been observed for SMMs in noncrystalline environments.[10] A preliminary account of this work has appeared in literature.[11]

Results and Discussion

Crystal structures: Figure 1 shows the molecular structures of complex **1**, $[Fe_4(acac)_6(Br\text{-}mp)_2]$ (acac = acetyl acetonate, Br-mpH_3 = 2-(bromomethyl)-2-(hydroxymethyl)-1,3-propanediol), and **2**, $[Fe^{III}_4(acac)_6(tmp)_2]$ (tmpH_3 = 2-ethyl-2-(hydroxymethyl)-1,3-propanediol), determined by X-ray crystallography. Both complexes crystallise in the monoclinic space group *C*2/*c*. The distorted octahedral coordination sphere of each of the peripheral iron ions is formed by two acac ligands and two oxygen atoms, one from each tripodal alkoxide. These alkoxide oxygen atoms form bridges to the central iron(III) ion, which is, therefore, coordinated by six of these atoms. The crystallographic structures of 14 tetranuclear iron(III) complexes with similar structures have been reported. Saalfrank et al. have employed derivatives of diethanolamine, $RN(CH_2CH_2OH)_2$ ($R = CH_3$, $PhCH_2$),[12,13] whereas Cornia et al. have been very successful with the complexes $[Fe_4(dpm)_6\{RC(CH_2O)_3\}_2]$, where dpm is deprotonated dipivaloyl methane and $R = CH_3$, $BrCH_2$, Ph, *t*Bu, *p*-ClPh or PhO.[14,15] Complexes **1** and **2** are very similar to these latter complexes, the only difference is that **1** and **2** feature acac instead of dpm ligands. The latter type of cluster was also modified for anchoring to surfaces and carbon nanotubes.[16] Further similar clusters include $[Fe_4(dpm)_6(OCH_3)_6]$,[17] $[Fe_4(n\text{PrOH})_6Cl_6\{CH_3C(CH_2O)_3\}_2]$,[18] and $[Fe_4(vap)_4(OCH_3)_4Cl_2]$ (vap = *o*-vanillinidene-3-propanolamine).[19]

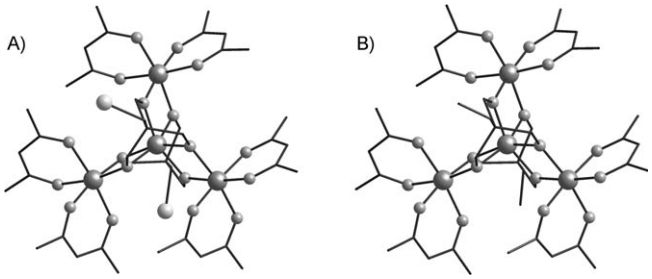

Figure 1. Molecular structures of compound **1** (A) and compound **2** (B). Iron ions are large, dark grey spheres, oxygen atoms are small spheres, and bromine atoms are large, light grey spheres. Carbon atoms are represented by sticks only, and hydrogen atoms have been omitted for clarity.

DC magnetic susceptibility: DC magnetic susceptibility data recorded for powder samples of **1** and **2** (Figure 2) show qualitatively the same behaviour. The observed room-temperature χT values (12.3 and 12.1 $cm^3\,K\,mol^{-1}$ for **1** and **2**, respectively) are significantly lower than those expected for four noninteracting high-spin iron(III) ions each with $S = 5/2$

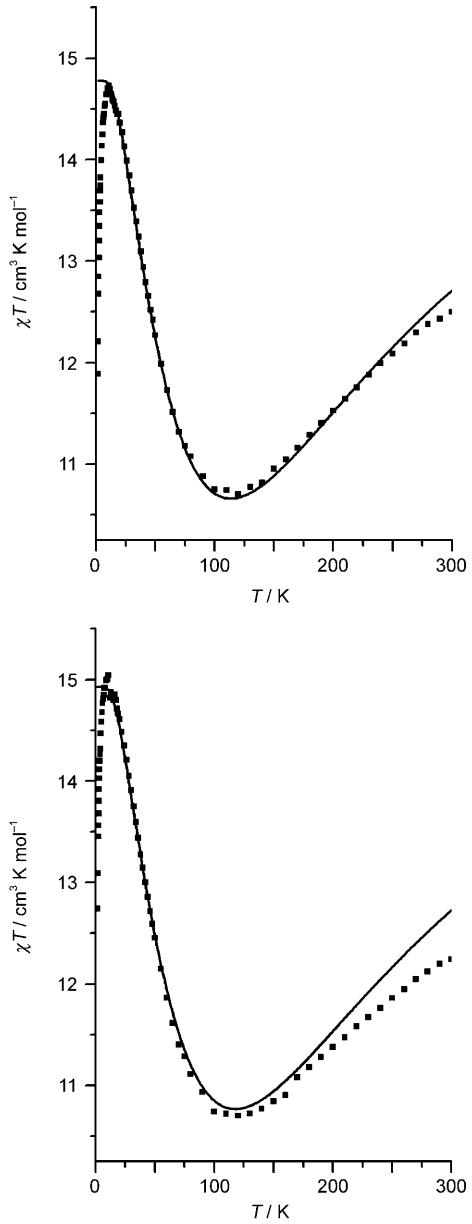

Figure 2. DC magnetic susceptibility–temperature product as a function of the temperature recorded for powder samples of **1** (top, ■) and **2** (bottom, ■). Solid lines are fits produced by using the Kambe model (see text; **1**: $J = -8.2\ cm^{-1}$, $g = 1.985$ and **2**: $J = -8.5\ cm^{-1}$, $g = 1.995$).

($17.5\ cm^3\,K\,mol^{-1}$ for $g=2.00$), indicating the presence of moderate antiferromagnetic exchange interactions, corroborated by the fact that the χT product decreases with decreasing temperature. However, at approximately 120 K, both curves reach a minimum beyond which the χT values rise again before they finally decrease below ≈ 15 K. Inspection of the structures (Figure 1) of the complexes reveals that antiferromagnetic nearest-neighbour interactions between the central spin and the peripheral spins will result in a non-zero-spin ground state. This ferrimagnetic structure accounts for the initial decrease in χT, followed by an increase to values close to that expected for an isolated $S=5$ state ($\chi T = 15\ cm^3\,K\,mol^{-1}$). The final decrease is due to zero-field splitting (ZFS) of the ground state or small intermolecular interactions. Considering nearest-neighbour superexchange interactions only, the isotropic exchange Hamiltonian is:

$$\mathrm{H} = -2J(\hat{\mathbf{S}}_1+\hat{\mathbf{S}}_2+\hat{\mathbf{S}}_3)\hat{\mathbf{S}}_4 \quad (1)$$

In view of the (idealised) trigonal symmetry of the complex, the susceptibility can be described analytically according to the Kambe formalism,[20] giving the following expression for the energies of the spin states at zero field:

$$E = J[S_{123}(S_{123}+1)-S_T(S_T+1)+S_4(S_4+1)] \quad (2)$$

where J is the exchange coupling strength, S_{123} the coupled spin of the peripheral ions, S_T the total spin and S_4 the spin of the central ion. A fit of J to the experimental data gives a value of $J=-8.2\ cm^{-1}$, with $g=1.985$ for compound **1**, and $J=-8.5\ cm^{-1}$, with $g=1.995$ for **2** (see Figure 2). This moderately strong exchange interaction leads to a well isolated $S=5$ ground multiplet, with the first excited multiplet ($S=4$) lying at approximately 60 K. These values are typical for Fe^{III}-O-Fe^{III} exchange interactions, and calculations according to published magneto–structural correlations give $J=-9.1\ cm^{-1}$ for **1** and $J=-9.4\ cm^{-1}$ for **2**.[21] The employed model does not reproduce the downturn in χT at lowest temperatures, which may be due to intermolecular interactions, next-nearest-neighbour intramolecular interactions and/or zero-field splitting of the ground state. Magnetisation measurements at variable temperatures and fields (not shown) show considerable nesting of the magnetisation curves, indicating the presence of significant anisotropy. Fits of the magnetisation curves, by employing the spin Hamiltonian $\mathrm{H}=D_{S=5}\hat{S}_z^2+ g\mu_B\mathbf{S}\cdot\mathbf{H}$, gave $D_{S=5}$ values of $-0.34\ cm^{-1}$, and $D_{S=5}=-0.35\ cm^{-1}$, for **1** and **2**, respectively.

AC magnetic susceptibility: The combination of a large-spin ground state and a negative D parameter suggests the possible occurrence of slow magnetisation dynamics or single-molecule magnet behaviour at low temperatures. Indeed, AC susceptibility measurements at temperatures $T \geq 1.8$ K show frequency dependent out-of-phase components χ''. However, the absolute value of the out-of-phase component is an order of magnitude smaller than the in-phase component and no maximum is observed. Hence, no distinction between possible sources of the observed slow magnetisation dynamics, including SMM behaviour, spin-glass-like behaviour, proximity to long-range ordering or phonon bottleneck effect, is possible. Therefore, we performed AC susceptibility measurements down to $T=90$ mK at frequencies up to 13333 Hz to investigate the origin of the observed slow relaxation behaviour (Figure 3). The results show clear, frequency-dependent maxima in the χ'' versus T curves. The shift in the temperature, T_f, of the maximum per decade in frequency, $\Delta T_f/[T_f\Delta\log(\omega)]$, is 0.25 for both complexes, which is a typical value for superparamagnet-like behaviour.[5] This shows that both molecules are single-molecule magnets, with relaxation times, τ, that can be described by the Arrhenius law $\tau=\tau_0\exp(\Delta E/k_BT)$, with ΔE being the energy barrier for the relaxation of the magnetisation and k_B being the Boltzmann constant. At T_f, $\omega\tau=1$, where $\omega=2\pi\nu_{AC}$, is the angular frequency corresponding to the driving frequency ν_{AC} of the AC susceptibility measurement. A linear fit of $\ln(\omega^{-1})$ versus T_f^{-1} (Figure 4) yields $\Delta E_{eff}=12.2\pm0.2$ K and $\tau_0=17\pm3$ ns for **1** and $\Delta E_{eff}=12.6\pm0.8$ K and $\tau_0=24\pm14$ ns for **2** (Table 1), which are the same within experimental accuracy. These energy-barrier values are identical to those calculated from the D values obtained from magnetisation measurements through $\Delta E=DS^2$. No evidence for deviation from linearity was observed in our data that span two decades in frequency. The frequency range is limited by the instrument on the high-frequency side and by a rapidly deteriorating signal-to-noise ratio on the low-frequency side. The application of a small field of 0.1 T increases the absolute relaxation times of **1**, but does not affect the temperature dependence (Figure 4), and a fit of the data yields $\Delta E_{eff}=12.4\pm0.4$ K and $\tau_0=47\pm12$ ns. This significant increase in τ_0 may be understood in terms of a decreased separation of the M_S states close to the top of the barrier, which slows down phonon-induced transitions between those states.[1]

Magnetic resonance: The experimental energy barriers to relaxation of the magnetisation, and the energy barriers calculated from $\Delta E=DS^2$ are identical, suggesting that (thermally activated) tunnelling is not a significant contributor to the magnetisation dynamics, and, hence, that transverse ZFS is negligible. To characterise the ZFS of the spin ground state more fully, we have recorded frequency-domain magnetic resonance (FDMR) spectra (Figure 5) and continuous-wave electron paramagnetic resonance (CW EPR; W-band) spectra (Figure 6). The FDMR spectra show single-magnetic resonance lines at 92 and 93 GHz for **1** and **2**, respectively, which are attributed to the $M_S=\pm5$ to $M_S=\pm4$ transitions within the respective ground state multiplets. The D values derived from these transition frequencies are $D_{S=5}=-0.34\ cm^{-1}$ for both compounds, in exact agreement with values derived from the magnetisation measurement. It is often the case with molecular clusters that the D values extracted from magnetisation measurements are unreliable due to the influence of excited spin states. For the present Fe_4 complexes, however, such states are energetically very

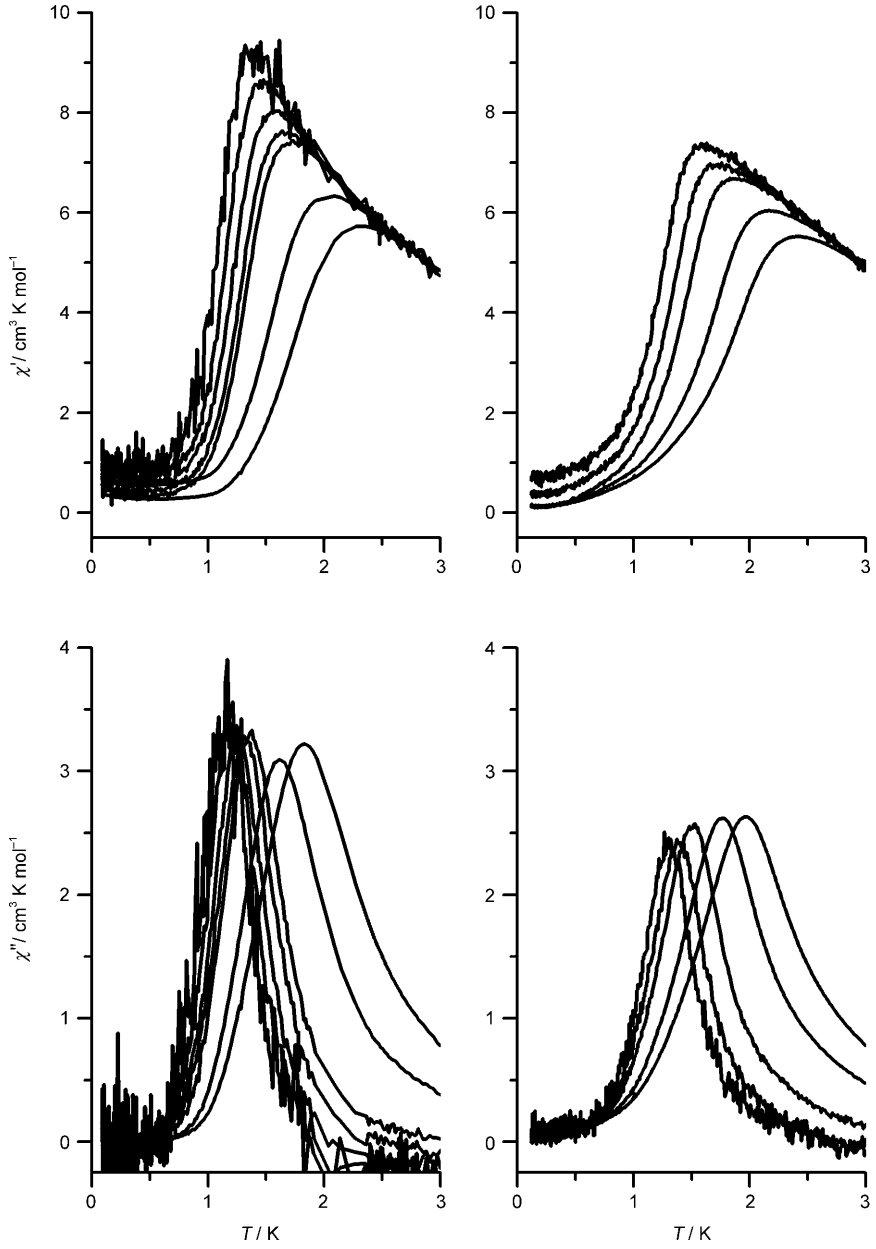

Figure 3. AC magnetic susceptibility–temperature product as a function of the temperature recorded for powder samples of **1** (left) and **2** (right), at frequencies from left to right: 251, 397, 629, 997, 1333, 5333 and 13333 Hz for **1**, and 333, 663, 1333, 5333, and 13333 Hz for **2**.

far from the ground multiplet, which accounts for the perfect agreement between magnetic resonance and magnetisation measurements for **1** and **2**. FDMR at these low frequencies is quite challenging with the wavelength ranging from 3–5 mm in the studied region, causing artefacts in the baseline due to standing waves. EPR is often more informative at these energies and indeed the W-band EPR spectrum (Figure 6A) recorded on a powder sample of **1** shows many more features. Extensive simulations revealed that the spectrum shows signatures of both D strain and partial orientation of the crystallites in the field. Although the space group is monoclinic, the two independent molecules in the unit cell have exactly the same orientation, leading to a strong tendency for the powder to orient. The best fit was obtained with the following parameters: $g=2.00$, $D_{S=5}=-0.342\pm0.002\ cm^{-1}$. Most Fe_4 stars possess $D_{S=5}$-values either in the range $-0.3 < D/cm^{-1} < -0.2$ or in the range $-0.5 < D/cm^{-1} < -0.4$ (Table 2). The intermediate values found for **1** and **2** are in good agreement with the "helical pitch", γ,[14] that is, the average dihedral angle formed between the plane through the four iron ions and the plane through the central and one of the peripheral iron ions and the two bridging oxygen atoms. It was shown that the $D_{S=5}$ value increases with helical pitch, where the γ values for **1** and **2** are intermediate between the two extremes found for the dpm complexes (Table 2). The last entry in Table 2 has a very small γ value in spite of a large $D_{S=5}$, but this complex has a different coordination sphere around the peripheral iron(III) ions (N_2O_4 vs. O_6), and the semiquantitative magnetostructural correlation cannot be expected to hold. Introduction of nonzero E, B_4^0 or B_4^3 values did not improve the simulated spectrum, which agrees with the fact that calculated (DS^2) and

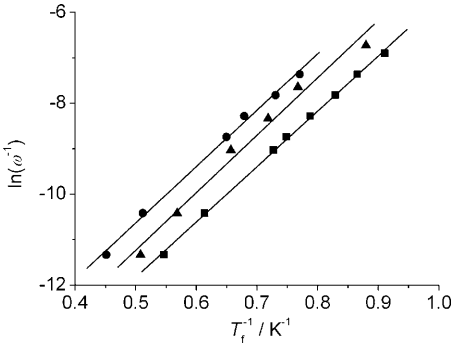

Figure 4. Plot of the natural logarithm of the inverse of the radial AC driving frequency as a function of the inverse of the temperature of the maximum in χ'' for the two compounds in 0 (■=**1** and ●=**2**) and 0.1 T (▲=**1**) applied fields. Drawn lines are linear fits.

Table 1. Experimental energy barriers and Arrhenius prefactors derived from AC susceptibility measurements.

Complex	Field [T]	Solid ΔE_{eff} [K]	Solid τ_0 [ns]	Solution ΔE_{eff} [K]	Solution τ_0 [ns]
1	0	12.2±0.2	17±3	12.0±0.3	280±40
	0.05			13.7±0.2	570±50
	0.10	12.4±0.4	47±12	14.1±0.3	630±70
	0.15			14.2±0.4	630±120
	0.20			13.8±0.4	800±130
2	0	12.6±0.8	24±14		

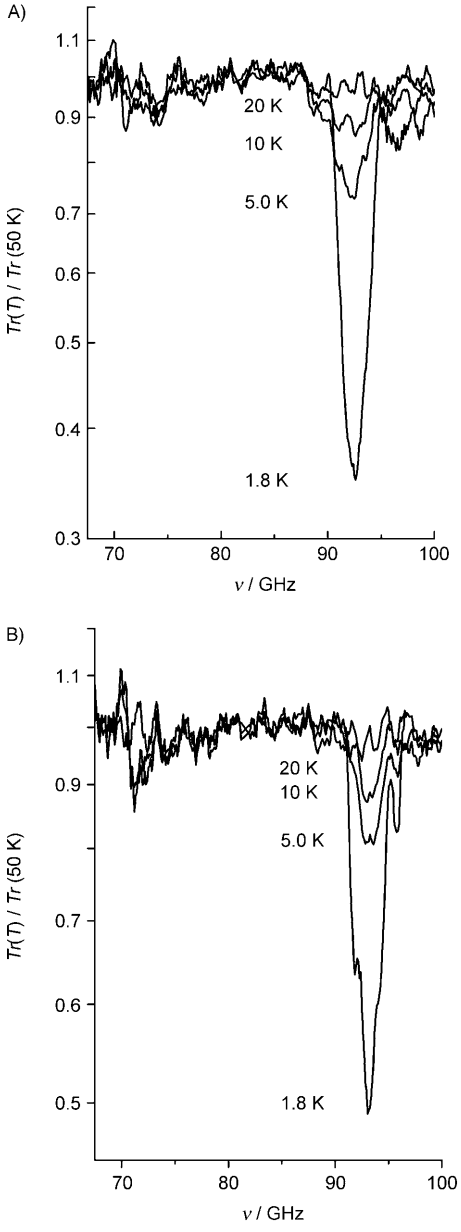

Figure 5. FDMR spectra recorded for pressed powder samples of **1** (A) and **2** (B) shown as normalised transmission as a function of frequency at different temperatures. Note that the 1.8 K spectra have been cropped to the region around the absorption lines, because of excessive baseline artefacts elsewhere due to the presence of liquid helium in the sample chamber.

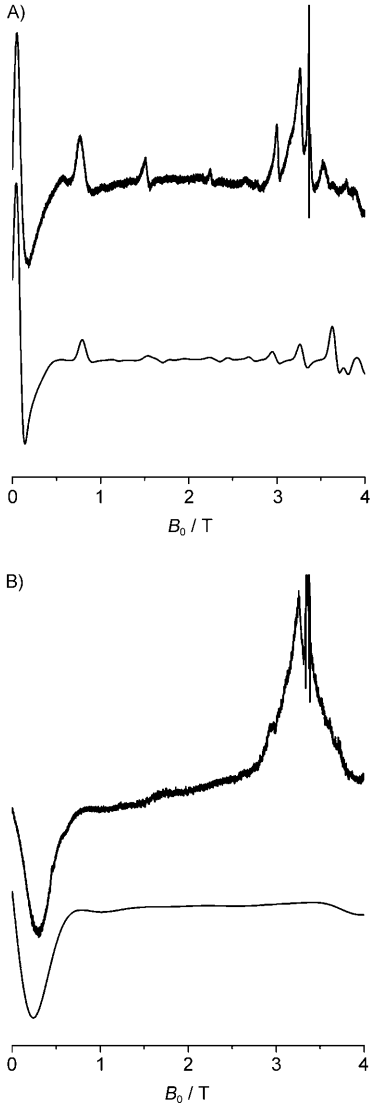

Figure 6. A) CW EPR (W-band) spectrum recorded for a powder sample of **1** at $\nu = 94.22$ GHz and $T = 4.3$ K (top) and fitted by using the parameters in the text (bottom). B) CW–EPR spectrum recorded for a frozen solution sample of **1** (0.5 mg mL^{-1} in toluene) at $\nu = 94.22$ GHz and $T = 4.5$ K (top) and fitted by using the parameters in the text (bottom).

effective energy barriers are equal, and tunnelling appears to play a minor role in these complexes.

Frozen-solution studies: The ultimate evidence for single-molecule magnet behaviour is the observation of slow relaxation of the magnetisation in diluted frozen solutions. None of the other physical phenomena that can lead to slow magnetisation dynamics persist in diluted solution. However, because molecular nanomagnets are often not the thermodynamically most stable product, they are not always stable in solution. Figure 7 shows the room-temperature, fluid solution ^{1}H NMR spectra of **1** in C_6D_6, recorded after different time delays. The NMR spectrum recorded for the freshly prepared solution shows peaks at $\delta = 44.2$, 20.3, 11 and −18.5 ppm. The second and fourth of these are attributed to

Table 2. Zero-field splitting parameters and ratios between experimental and calculated (on the basis of the ZFS parameters) energy barriers towards relaxation of the magnetisation derived for **1** and **2**, and comparison with similar complexes.

Complex	D [cm^{-1}]	B_4^0 [10^{-5} cm^{-1}]	$\Delta E_{eff}/DS^2$[a]	γ [°][b]
1	-0.342 ± 0.002	0	0.99 ± 0.01	66.4
2	-0.35 ± 0.01	0	1.00 ± 0.03	66.0
$[Fe_4(dpm)_6(OCH_3)_6]$[17]	−0.206	−1.1	0.47	63.2
$[Fe_4(dpm)_6\{CH_3C(CH_2O)_3\}_2]$[17]	−0.445	+1.0	1.06	70.8
$[Fe_4\{RN(CH_2CH_2O)_2\}_6]$[12]	−0.40	−2.1	n/a	60.5

[a] Note that $\hat{O}_4^0(|SM_S>=|5\pm5>)-\hat{O}_4^0(|5\pm0>)=0$, hence, the theoretical energy barrier is independent of B_4^0; [b] γ is the helical pitch, defined in [14].

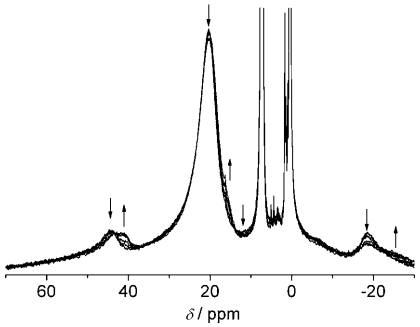

Figure 7. ^1H NMR spectra recorded for a solution of **1** in C_6D_6 at room temperature at various times after preparation (0, 30, 90, 405, 1440, 3000 min). Arrows indicate appearing and disappearing peaks.

the methyl and methine protons of the acac ligand, respectively.[22] The remaining peaks are assigned to the Fe–OCH_2– and –CH_2Br moieties, respectively. Over time, the intensity of all these peaks decreases, whereas new peaks appear, at $\delta=41.1$, 16.0 and −25.1 ppm, indicating that the complex decomposes over time. Possible decomposition products include $[Fe(acac)_3]$, similar to what has been reported for $[Fe_4(L)_2(dpm)_6]$ clusters.[14] No extensive decomposition has taken place after 30 min and all sample preparations for subsequent measurements were completed within that period. In addition, magnetic measurements were repeated after 24 h to ensure that the measurement results were not due to decomposition products. CW EPR (W-band) spectra were recorded for characterisation of the ZFS of the ground state (Figure 6B), and a satisfactory fit of the spectrum was obtained with $D=-0.35\pm0.01$ cm^{-1}, and a line width of 0.5 ± 0.1 T. The large line width prevented more accurate characterisation of the ZFS.

AC susceptibility measurements on a frozen solution of 1 in toluene (5.0 mg mL^{-1}, Figure 8) reveal that the onset of out-of-phase signals occurs at higher temperatures for a given frequency, than found for polycrystalline samples of the same material (Figure 3). In addition, the maxima in the out-of-phase component of the AC susceptibility shift to higher temperatures upon the application of an external DC field. Measurements at lower concentrations (0.5 mg mL^{-1}) did not yield significantly different results indicating that intermolecular magnetic dipolar interactions play a minor role in the magnetisation dynamics. Fits of $\ln(\tau)$ as a function of $1/T$ yield the energy barriers and pre-exponential factors at various external fields (Table 1). These data demonstrate that the energy barrier in a zero field is unchanged compared to the solid state, and shows a small and probably insignificant increase upon application of an external field. More striking is the change in the pre-exponential factor τ_0, which increases by an order of magnitude going from the solid state to solution. In these measurements the accessible frequency range was limited by the instrument of the high-frequency side and by the base temperature on the low-frequency side. This means that the data do not allow the detection of small deviations from the Arrhenius law. Measurements at higher

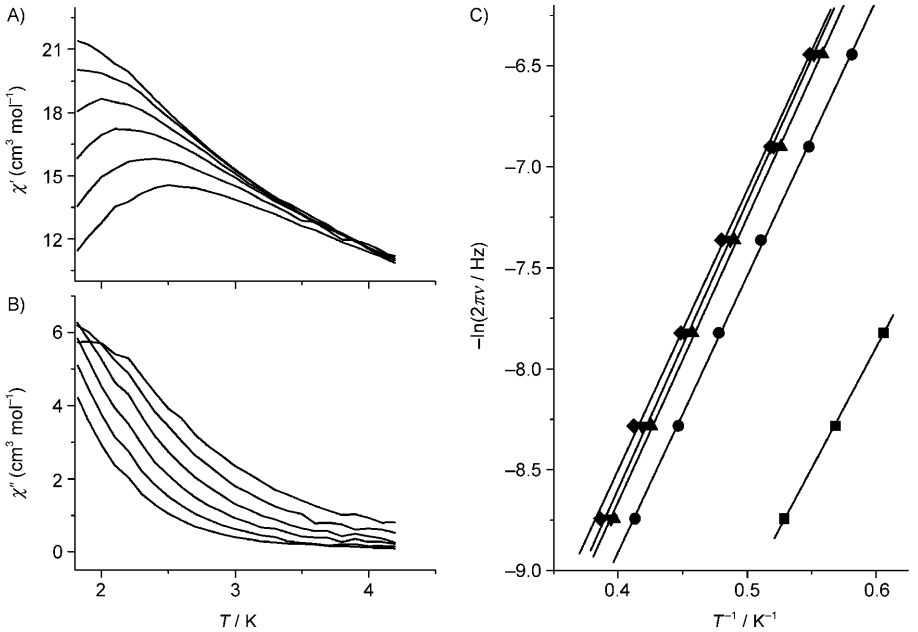

Figure 8. A) In-phase and B) out-of-phase component of the AC susceptibility recorded for a solution of **1** in toluene (5.0 mg mL^{-1}) at 0 T. Frequencies from top to bottom (A) or from left to right (B): 100, 158, 251, 397, 629, 997 Hz. C) Relaxation times and temperatures derived from Lorentz fits of the out-of-phase components of the AC susceptibility measurements at different external magnetic fields (■ = 0 T, ● = 0.05 T, ▲ = 0.1 T, ▼ = 0.15 T and ◆ = 0.2 T).

frequencies were not possible, because the high-frequency susceptometer does not accommodate frozen-solution samples. However, the change in τ_0 is by an order of magnitude, which is clear even in the limited frequency range studied. Clearly, it is this difference that causes the observed increase in relaxation time. Interestingly, the observed increase in τ_0 leads to a twofold increase in blocking temperature at a given measurement time scale. The τ_0 factor depends on several contributions, including the strength of the spin–phonon coupling, the speed of sound and the density of acoustic phonons, all of which may change depending on the matrix in which the individual molecules are incorporated.[1] In addition to the change in medium itself, the intermolecular dipolar interactions will be strongly decreased going from the solid state to a frozen solution. This may be expected to have a significant influence on the magnetisation dynamics and quantum tunnelling. For ground-state tunnelling (which is temperature-independent) this might actually lead to an apparent change in τ_0, but not for thermally assisted tunnelling (which is temperature-dependent).

Conclusion

We have described the magnetic properties of two novel Fe_4 star-shaped single-molecule magnets. Their magnetic anisotropies are in between that found for related complexes, and correlate well with structural parameters. Interestingly, the magnetisation relaxation time increases on going from the solid state to solution, which was shown to originate from an increase in the pre-exponential factor in the Arrhenius relation. This study demonstrates that control of this factor is as yet an unexplored factor to tune and improve single-molecule magnet properties. Further investigation into the precise origin of the τ_0 factor is clearly warranted.

Experimental Section

$[Fe_4(acac)_6(Br\text{-}mp)_2]$ (1): $[Fe(acac)_2]$ (500 mg, 1.97 mmol) and Br-mpH_3 (392 mg, 1.97 mmol) in MeCN (25 mL) in the presence of NaN_3 (128 mg, 1.97 mmol) and NaOMe (106 mg, 1.97 mmol) were stirred at room temperature for 14 h, followed by slow evaporation of the solvent to afforded orange crystals of **1** during 8 days in a yield of ≈40%. Elemental analysis calcd (%) for $C_{40}H_{58}Br_2Fe_4O_{18}$: C 39.70%, H 4.83%; found: C 39.84%, H 4.48%.

$[Fe^{III}_4(acac)_6(tmp)_2]$ (2): In an analogous manner to the preparation of **1** by replacing Br-mpH_3 with tmpH_3 orange crystals of **2** were prepared in a yield of ≈40%. Elemental analysis calcd (%) for $C_{42}H_{64}Fe_4O_{18}$: C 46.69%, H 5.93%; found: C 46.55%, H 5.75%.

Crystallography: Crystallographic data for **1** and **2** were measured on a Bruker SMART Apex CCD detector diffractometer by using graphite-monochromated $Mo_{K\alpha}$ radiation ($\lambda = 0.71073$ Å). The structures were solved by Patterson and direct methods, respectively, and refined by full-matrix least squares against F^2 for all data by using the SHELXTL software package.[23] All non-hydrogen atoms were refined anisotropically; Hydrogen atoms were placed in calculated positions. CCDC-717578 and 717579 contain the supplementary crystallographic data for this paper. These data can be obtained free of charge from The Cambridge Crystallographic Data Centre via www.ccdc.cam.ac.uk/data_request/cif.

Physical measurements: DC and AC magnetic susceptibility and DC magnetisation data were obtained on Quantum Design MPMS XL7 magnetometers. Low- and ultralow-temperature AC data were recorded on Quantum Design PPMS and homebuilt AC-susceptometers.[24] To prevent crystallisation of the compound, toluene solutions for AC measurements (5.0 mg mL^{-1}) were quench-cooled from room temperature to 4 K, by rapid insertion of the sample rod into the SQUID magnetometer. Frequency domain magnetic resonance measurements were performed as previously described,[25] whereas a Bruker Elexsys E680 spectrometer was employed for CW EPR (W-band) measurements. EPR spectra were simulated by using the Easyspin package.[26] Solution NMR spectra were recorded on a Bruker DPX300 spectrometer

Acknowledgements

We acknowledge funding from the Deutsche Forschungsgemeinschaft (DFG), the DAAD (Acciones Integradas) the EPSRC (EP/G004757/1), the Royal Society, the Leverhulme Trust, the Spanish MICINN (grant MAT2009-13977-C03-01) and DGA (grant PI091/08). Prof. Mehring and Prof. Denninger (Stuttgart) are thanked for use of their EPR spectrometer. Prof. Martin Dressel is thanked for useful discussions.

[1] D. Gatteschi, R. Sessoli, J. Villain, *Molecular Nanomagnets*, Oxford University Press, Oxford, **2006**.
[2] F. Luis, J. Campo, J. Gómez, G. J. McIntyre, J. Luzón, D. Ruiz-Molina, *Phys. Rev. Lett.* **2005**, *95*, 227202.
[3] F. Luis, J. Bartolome, J. F. Fernandez, *Phys. Rev. B* **1998**, *57*, 505–513.
[4] E. C. Yang, W. Wernsdorfer, L. N. Zakharov, Y. Karaki, A. Yamaguchi, R. M. Isidro, G. D. Lu, S. A. Wilson, A. L. Rheingold, H. Ishimoto, D. N. Hendrickson, *Inorg. Chem.* **2006**, *45*, 529–546.
[5] J. A. Mydosh, *Spin Glasses: An Experimental Introduction*, Taylor & Francis, London, **1993**, p. 256.
[6] N. Lopez, A. V. Prosvirin, H. Zhao, W. Wernsdorfer, K. R. Dunbar, *Chem. Eur. J.* **2009**, *15*, 11390–11400.
[7] D. Gatteschi, A. Cornia, M. Mannini, R. Sessoli, *Inorg. Chem.* **2009**, *48*, 3408–3419.
[8] M. Mannini, F. Pineider, P. Sainctavit, C. Danieli, E. Otero, C. Sciancalepore, A. M. Talarico, M. A. Arrio, A. Cornia, D. Gatteschi, R. Sessoli, *Nat. Mater.* **2009**, *8*, 194–197.
[9] C. Schlegel, J. van Slageren, M. Manoli, E. K. Brechin, M. Dressel, *Phys. Rev. Lett.* **2008**, *101*, 147203; S. Takahashi, J. van Tol, C. C. Beedle, D. N. Hendrickson, L. C. Brunel, M. S. Sherwin, *Phys. Rev. Lett.* **2009**, *102*, 087603; G. Aromí, E. Bouwman, E. Burzurí, C. Carbonera, J. Krzystek, F. Luis, C. Schlegel, J. van Slageren, S. Tanase, S. J. Teat, *Chem. Eur. J.* **2008**, *14*, 11158.
[10] H. J. Eppley, H. L. Tsai, N. Devries, K. Folting, G. Christou, D. N. Hendrickson, *J. Am. Chem. Soc.* **1995**, *117*, 301–317; R. Sessoli, *Mol. Cryst. Liq. Cryst.* **1995**, *274*, 145–157; A. Caneschi, T. Ohm, C. Paulsen, D. Rovai, C. Sangregorio, R. Sessoli, *J. Magn. Magn. Mater.* **1998**, *177–181*, 1330–1336; A. Naitabdi, J. P. Bucher, P. Gerbier, P. Rabu, M. Drillon, *Adv. Mater.* **2005**, *17*, 1612–1616; F. El Hallak, J. van Slageren, J. Gomez-Segura, D. Ruiz-Molina, M. Dressel, *Phys. Rev. B* **2007**, *75*, 104403; I. Imaz, F. Luis, C. Carbonera, D. Ruiz-Molina, D. Maspoch, *Chem. Commun.* **2008**, 1202–1204; N. Domingo, F. Luis, M. Nakano, M. Munto, J. Gomez, J. Chaboy, N. Ventosa, J. Campo, J. Veciana, D. Ruiz-Molina, *Phys. Rev. B* **2009**, *79*, 214404; C. Carbonera, J. Sánchez-Marcos, A. Camón, J. Chaboy, D. Ruiz-Molina, J. van Slageren, S. Dengler, M. González, *Phys. Rev. B* **2010**, *81*, 014427.
[11] C. Schlegel, J. van Slageren, M. Manoli, E. K. Brechin, M. Dressel, *Polyhedron* **2009**, *28*, 1834–1837.
[12] R. W. Saalfrank, A. Scheurer, I. Bernt, F. W. Heinemann, A. V. Postnikov, V. Schunemann, A. X. Trautwein, M. S. Alam, H. Rupp, P. Muller, *Dalton Trans.* **2006**, 2865–2874.

[13] R. W. Saalfrank, I. Bernt, M. M. Chowdhry, F. Hampel, G. B. M. Vaughan, *Chem. Eur. J.* **2001**, *7*, 2765–2769.
[14] S. Accorsi, A. L. Barra, A. Caneschi, G. Chastanet, A. Cornia, A. C. Fabretti, D. Gatteschi, C. Mortalò, E. Olivieri, F. Parenti, P. Rosa, R. Sessoli, L. Sorace, W. Wernsdorfer, L. Zobbi, *J. Am. Chem. Soc.* **2006**, *128*, 4742–4755.
[15] A. Cornia, A. C. Fabretti, P. Garrisi, C. Mortalò, D. Bonacchi, D. Gatteschi, R. Sessoli, L. Sorace, W. Wernsdorfer, A. L. Barra, *Angew. Chem.* **2004**, *116*, 1156–1159; *Angew. Chem. Int. Ed.* **2004**, *43*, 1136–1139; G. G. Condorelli, A. Motta, G. Pellegrino, A. Cornia, L. Gorini, L. L. Fragala, C. Sangregorio, L. Sorace, *Chem. Mater.* **2008**, *20*, 2405–2411.
[16] A. L. Barra, F. Bianchi, A. Caneschi, A. Cornia, D. Gatteschi, L. Gorini, L. Gregoli, M. Maffini, F. Parenti, R. Sessoli, L. Sorace, A. M. Talarico, *Eur. J. Inorg. Chem.* **2007**, 4145–4152; L. Bogani, C. Danieli, E. Biavardi, N. Bendiab, A. L. Barra, E. Dalcanale, W. Wernsdorfer, A. Cornia, *Angew. Chem.* **2009**, *121*, 760; *Angew. Chem. Int. Ed.* **2009**, *48*, 746.
[17] A. L. Barra, A. Caneschi, A. Cornia, F. Fabrizi de Biani, D. Gatteschi, C. Sangregorio, R. Sessoli, L. Sorace, *J. Am. Chem. Soc.* **1999**, *121*, 5302–5310.
[18] M. Moragues-Cánovas, P. Rivière, L. Ricard, C. Paulsen, W. Wernsdorfer, G. Rajaraman, E. K. Brechin, T. Mallah, *Adv. Mater.* **2004**, *16*, 1101–1105.
[19] N. T. Madhu, J. K. Tang, I. J. Hewitt, R. Clerac, W. Wernsdorfer, J. van Slageren, C. E. Anson, A. K. Powell, *Polyhedron* **2005**, *24*, 2864–2869.
[20] K. Kambe, *J. Phys. Soc. Jpn.* **1950**, *5*, 48.
[21] C. Cañada-Vilalta, T. A. O'Brien, E. K. Brechin, M. Pink, E. R. Davidson, G. Christou, *Inorg. Chem.* **2004**, *43*, 5505–5521.
[22] H. Kobayashi, H. Matsuzawa, Y. Kaizu, A. Ichida, *Inorg. Chem.* **1987**, *26*, 4318–4323.
[23] Shelxtl 5.1, G. M. Sheldrick, Madison WI, **1997**.
[24] A. Morello, F. L. Mettes, O. N. Bakharev, H. B. Brom, L. J. de Jongh, F. Luis, J. F. Fernandez, G. Aromí, *Phys. Rev. B* **2006**, *73*, 134406.
[25] J. van Slageren, S. Vongtragool, B. Gorshunov, A. A. Mukhin, N. Karl, J. Krzystek, J. Telser, A. Muller, C. Sangregorio, D. Gatteschi, M. Dressel, *Phys. Chem. Chem. Phys.* **2003**, *5*, 3837–3843.
[26] S. Stoll, A. Schweiger, *J. Magn. Reson.* **2006**, *178*, 42–55.

Received: December 21, 2009
Revised: April 23, 2010
Published online: July 9, 2010

